

Large Eddy Simulation of turbulent lifted flame

M. Mortada and C. B. Devaud*

*Department of Mechanical and Mechatronics Engineering, University of Waterloo, 200 University Avenue
West, Waterloo, ON, Canada, N2L3G1*

Abstract

Turbulent lifted flames are found in the combustion process of gas turbines, diesel engines, and direct fuel injection gasoline engines which involve stratified mixtures. The objectives of the current work are to perform Large Eddy Simulation (LES) of a turbulent lifted methane flame surrounded by quiescent cold air and investigate different numerical parameters and submodels for most accurate predictions of flame stabilization. The Doubly Conditional Source-term Estimation (DCSE) method is used to close the chemical source term in the species conservation equation. A constant Smagorinsky model is applied. Detailed chemistry is included, and tabulated using Trajectory Generated Low Dimensional Manifold (TGLDM). The computations are run using OpenFOAM. LES-DCSE is successful in reproducing the turbulent lifted flame with good predictions of methane concentration profiles. An over-prediction of lift-off height and methane concentration fluctuations is observed. The scalar dissipation rate model is shown to have an impact on the reacting predictions.

1 Introduction

Although numerical modelling of reactive turbulent flows has been proved to be less expensive than the experimental approach in describing combustion systems and providing detailed insight into the involved physical processes, turbulent combustion modelling faces a number of challenges to provide an accurate prediction of flames. In particular, the main challenge is the closure of the mean chemical source-term due to the high non-linearity of the chemical reaction rates. One of the flames that captured the interest in combustion research is the lifted jet flame. The phenomenon of flame lift-off is observed when the flame stabilizes at a distance away from the nozzle exit which is defined as the lift-off height [1]. Many theories have been investigated to describe the lifted flame stabilization mechanism. One of the early approaches is the premixed flame propagation theory: the flame base stabilizes itself at the location where the burning velocity is equal to the mean flow velocity. Although this theory is supported by some experimental findings [2, 3], it has been questioned [4, 5]. Another theory is the critical scalar dissipation rate (SDR) concept [6]. It assumes that the reaction zone is displaced downstream and stabilizes at the location of the critical low value of SDR. One of the flaws is that it ignores the mixing that takes place upstream of the flame base [1, 3, 4]. The third approach assumes that the large vortices entrain the hot products into the edge of the jet to ignite the combustible mixture [7]. However, this model is not consistent with some experimental studies [4]. In the current work, the partially premixed flame propagation is considered, which is supported by recent experimental investigations [5, 8] which include both premixed and non-premixed flames. This modelling strategy is first investigated in the context of flamelet model [9]. The agreement between the predicted lift-off heights and the experimental data is reasonable but the model tends to be fully premixed most of the time. Another formulation based on two scalars, mixture fraction and G , is proposed by Müller et al. [10]. The G -equation is used to describe the flame propagation with the laminar burning velocity as a function of mixture fraction. The main issue is related to the turbulent burning velocity closure. Due to additional closed terms, no fully coupled partially premixed formulation in CMC. However, some *a priori* tests using DNS can be found [11]. The Conditional Source-term Estimation (CSE) model has been modified for the first time by Dovizio et al. [12] to describe partially premixed flame propagation through two conditioning variables: the mixture fraction and the reaction progress variable. A series of lifted flames are investigated in RANS using a simple model for the SDR. Further, DCSE is used successfully to model several

*Corresponding author: cdevaud@uwaterloo.ca

turbulent stratified V-shaped flames in RANS [13, 14]. As a starting point in the present study, the lowest Re flame is the flame investigated due to availability of experimental data. The objective of the present paper is to numerically investigate the low Reynolds number turbulent jet lifted flame [15] using Large Eddy Simulation (LES). The investigation includes an assessment of the ability of DCSE in reproducing the turbulent lifted flame, and comparing the reacting predictions obtained using different SDR models.

2 DCSE formulation

2.1 DCSE principle

CSE is proposed by Bushe and Steiner [16]. It is based on the principle that the fluctuations about the conditional means are negligible compared to the fluctuations about the unconditional means. DCSE uses mixture fraction and reaction progress variable as conditioning variables. The unconditional filtered chemical source-term for species k , $\overline{\dot{\omega}_k}$ is obtained by integrating the conditional filtered chemical source-term multiplied by the joint Filtered Density Function (FDF) over both mixture fraction and reaction progress variable spaces as follows

$$\overline{\dot{\omega}_k}(x_j, t) = \int_0^1 \int_0^1 \overline{\dot{\omega}_k | \eta, c^*}(x_j, t) \overline{P}(\eta, c^*, x_j, t) d\eta dc^*. \quad (1)$$

The joint PDF is obtained using the following expression [17]: $\tilde{P}(\eta, c^*) = \tilde{P}(\eta) \tilde{P}(c^* | \eta)$ where $\tilde{P}(\eta)$ is calculated using the distribution of β -PDF [18], and $\tilde{P}(c^*)$ calculated using the unstrained laminar premixed flame [19]. For some fuel lean and rich conditions, the β -PDF is used for $\tilde{P}(c^* | \eta)$ instead of the unstrained laminar premixed flame outside the flammability limits. The conditional averages are shown to vary much less in space compared to the unconditional averages [20]. Thus, the conditional averages are considered space invariant for each ensemble of points and discretized as

$$\tilde{f}(\vec{x}_j, t) = \int_{\eta_1}^{\eta_2} \int_{c^*_1}^{c^*_2} \overline{f | \eta, c^*}(\eta, c^*; t) \tilde{P}(\eta_m, c^*_m; \vec{x}_j, t) d\eta dc^*, \quad (2)$$

where m indicates the index of the sample point within the sample interval (bin), and $\eta_1, \eta_2, c^*_1, c^*_2$ are the lower and upper bounds of the bin for mixture fraction and progress variable, respectively. In the case of DCSE, the combined mixture fraction/progress variable space is composed of $(n_\eta \times n_c)$ points where n_η is the number of points in mixture fraction space and n_c the number of points in the progress variable space. Equation 2 can be cast in matrix form as $\mathbf{A} \vec{\alpha} = \vec{b}$ where \mathbf{A} is a $(N \times M)$ matrix where N is the number of grid points in the ensemble and M the number of bins in the combined mixture fraction/progress variable space, $\vec{\alpha}$ is the conditional averaged scalar vector of size M for a given ensemble, and \vec{b} is the unconditional averaged scalar vector of size N . Matrix \mathbf{A} represents the integrated joint PDF which is a function of mixture fraction and progress variable as well as space and time. The solution for $\vec{\alpha}$ is ill-posed. Therefore, it is sensitive to small perturbations. To get a unique smooth solution, regularization is required. The regularization approach involves solving the minimization problem:

$$\vec{\alpha} = \arg \min \left\{ \left\| \mathbf{A} \vec{\alpha} - \vec{b} \right\|_2 + \lambda^2 \left\| \vec{\alpha} - \vec{\alpha}_0 \right\|_2 \right\}, \quad (3)$$

where $\|\cdot\|_2$ represents L2-norm, λ is the regularization parameter, $\vec{\alpha}_0$ the *a priori* knowledge which is often selected as the solution from the previous time-step. The Least-Squares QR-factorization (LSQR) algorithm is used to solve the system of over-determined least squares in Eq. 3.

2.2 Transport equations

The solution procedure includes solving the transport equations of mass, momentum, enthalpy and species. The distribution of mixture fraction and a reaction progress variable characterizes the partially premixed flame. The mixture fraction is defined as a ratio that represents the degree of mixing of fuel and the oxidizer. This ratio takes values from 0 at pure oxidizer case, to 1 at pure fuel case. In the present calculations, transported equations for resolved mixture fraction, \tilde{Z} , and its SGS variance, $\widetilde{Z''^2}$, are solved. The reaction progress variable represents the degree of consumption of the fuel. It has values that range from zero in fresh gas (with no products) to unity for the completely burnt gases (with no reactants presented at that location). In the present work, the progress

variable is defined as $c(Z) = Y_{CO_2}/Y_{CO_2}^{Eq}(Z)$, where $Y_{CO_2}^{Eq}(Z)$ is the equilibrium value of the mass fraction of carbon dioxide (CO₂) which is ideally obtained when complete combustion takes place, which is a function of equivalence ratio. The transport equations of filtered progress variable and its variance are included. The governing equation of the SGS variance of reaction progress variable is

$$\frac{\partial(\overline{\rho c''^2})}{\partial t} + \frac{\partial}{\partial x_i}(\overline{\rho \tilde{u}_i c''^2}) = - \underbrace{\frac{\partial}{\partial x_i}(\overline{\rho u_i'' c''^2})}_{\text{turbulent transport}} + \underbrace{\frac{\partial}{\partial x_i}(\overline{\rho D \frac{\partial c''^2}{\partial x_i}})}_{\text{molecular diffusion}} - \underbrace{2\overline{\rho u_i'' c''}}_{\text{production}} - \underbrace{\overline{\rho D \frac{\partial c''}{\partial x_i} \frac{\partial c''}{\partial x_i}}}_{\text{dissipation}} + \underbrace{\overline{2c'' \dot{\omega}_c}}_{\text{source-term}}. \quad (4)$$

2.3 The scalar dissipation rate (SDR) model

A simple algebraic model, initially developed in RANS [21], is adapted to LES as

$$\tilde{\chi}_c = C_\chi (\tilde{\epsilon}_{sgs}/\tilde{k}_{sgs}) \tilde{c}''^2, \quad (5)$$

where a value of 1 is used for the constant C_χ similar to the value used in RANS. The SGS dissipation rate is calculated internally by OpenFOAM using $\tilde{\epsilon}_{sgs} = c_\epsilon \tilde{k}_{sgs} \sqrt{\tilde{k}_{sgs}}/\Delta$, where c_ϵ is a model constant with a default value of 0.202, Δ the filter size, calculated using the cube root volume, $\Delta = (\Delta x \Delta y \Delta z)^{\frac{1}{3}}$ with Δx , Δy and Δz being the grid spacing in Cartesian coordinates. In the RANS framework, an advanced algebraic model is derived by Kolla et al. [22] for high Damköhler number by balancing the leading order terms defined by means of order of magnitude analysis. In comparison with DNS data, the model shows good predictions of the scalar dissipation rate values. This is explained by the fact that the effect of dilatation, strain due to heat release, and the turbulent mixing time are included. The model is extended by Dovizio et al. [14] for turbulent partially premixed flame. The algebraic expression is given as a function of the mixture fraction and adapted to LES as follows

$$\tilde{\chi}_c(\tilde{Z}) = 2\bar{\rho} \frac{1}{\beta'} \left(2K_{c^*}(\tilde{Z}) \frac{S_L(\tilde{Z})}{\delta_L(\tilde{Z})} - \tau(\tilde{Z}) C_4(\tilde{Z}) \frac{S_L(\tilde{Z})}{\delta_L(\tilde{Z})} \right) + C_3(\tilde{Z}) \frac{\tilde{\epsilon}_{sgs}}{\tilde{k}_{sgs}} \tilde{c}''^2. \quad (6)$$

where β' is model constant which is taken as 6.7, τ heat release parameter and K_{c^*} a model constant. Selected values for τ and K_{c^*}/τ correspond to the selected value of mixture fraction. The other model constants C_3 and C_4 are calculated as a function of Karlovitz number.

2.4 Trajectory-Generated Low Dimensional Manifold (TGLDM)

For methane-air combustion, GRI-MECH 2.11 is the used detailed mechanism in the current study. It includes 49 species and 277 elementary reactions. Due to high computational cost, a dimension reduction and tabulation method is adopted for the current work, which is the Trajectory Generated Low Dimensional Manifold (TGLDM), proposed by Pope and Maas [23]. Different manifolds are defined depending on the number of reduced dimensions. The manifold is comprised of reaction trajectories that are generated from the boundaries of the manifold. The resulting chemistry tables include four dimensions η , c^* , Y_{CO_2} and Y_{H_2O} . The mass fractions of CO₂ and water (H₂O) are selected to be the variables by which the resulted manifolds are stored in the form of structured tables. This selection is made because the formation time of carbon dioxide and water is relatively long compared to the other species.

3 Computational Details

3.1 Experimental case

The experimental setup involved in the current investigation is simply a fuel jet of 5.4 mm diameter surrounded by approximately quiescent ambient air. The velocity provided for the fuel jet has an average value of 21 m/s corresponding to a jet Reynolds number of 7,000 [15].

3.2 Numerical implementation

The governing transport equations are solved using a finite volume low-Mach number pressure based approach. The employed solver is the open source CFD package of OpenFOAM using PISO algorithm for pressure corrections. The solution schemes are second order in time and space. A constant Smagorinsky model is used.

The computational domain is built in the form of a cylinder of radius 189 mm and height of 540 mm. A grid sensitivity analysis is performed for 3 grids comprised of 798,000, 3,232,000 and 7,965,000 cells. The second grid is selected to provide the final results, while some preliminary reacting predictions are obtained for the first grid. The quality of each grid is assessed based on the resolved kinetic energy and comparison with experimental data, not shown here for brevity. At the fuel inlet, a velocity profile is set using the one seventh law and a decaying turbulence inflow generator is applied.

3.3 DCSE ensembles

To define the DCSE ensembles, the ensemble selection not only involves radial divisions using planes normal to the centreline but also includes dividing each radial plane into quarters to make sure that the number of reactive cells per ensemble is not below $(n_z \times n_c)$ and not too high, to keep the PDF matrix and the unconditional means vector at a reasonable size. The number of ensembles used is 24 ensembles.

4 RESULTS

The methane concentration is evaluated as the measured methane number density normalized by the number density of pure methane at standard conditions of temperature and pressure. This normalizing value is provided as $(2.5 \times 10^{19} \text{ molecules/cm}^3)$ [15].

4.1 Non-reacting predictions

Time-averaged statistics are determined over 57 flow through times. The predicted time-averaged methane concentration profiles obtained by grid 2 are presented in Fig.1. Good agreement between the experimental

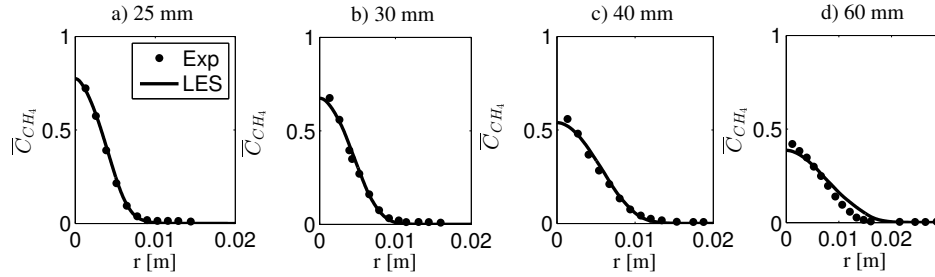


Fig. 1: Non-reacting methane mean concentration profiles at different axial positions downstream of the jet

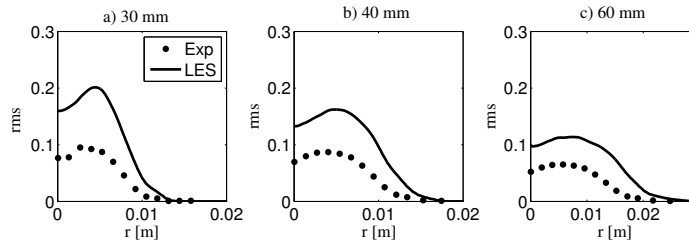


Fig. 2: Non-reacting methane rms concentration profiles at different axial positions downstream of the jet

data and the mean methane concentration profiles is reached. However, there is a significant over-prediction of the fluctuations of the methane concentration radial profiles, as shown in Fig. 2 where the fluctuations are defined as the root mean square of methane concentrations. This may be due to some assumptions used for Re stresses at the fuel inlet.

4.2 Reacting predictions

Simulations are still in progress for grid 2. Thus, as a first step, the predictions from grid 1 are shown. To assess the effect of the SDR model, two identical cases are run with different SDR models; One uses the simple

algebraic model (Eq. 5) and the other includes the advanced algebraic model (Eq. 6). For both cases, the

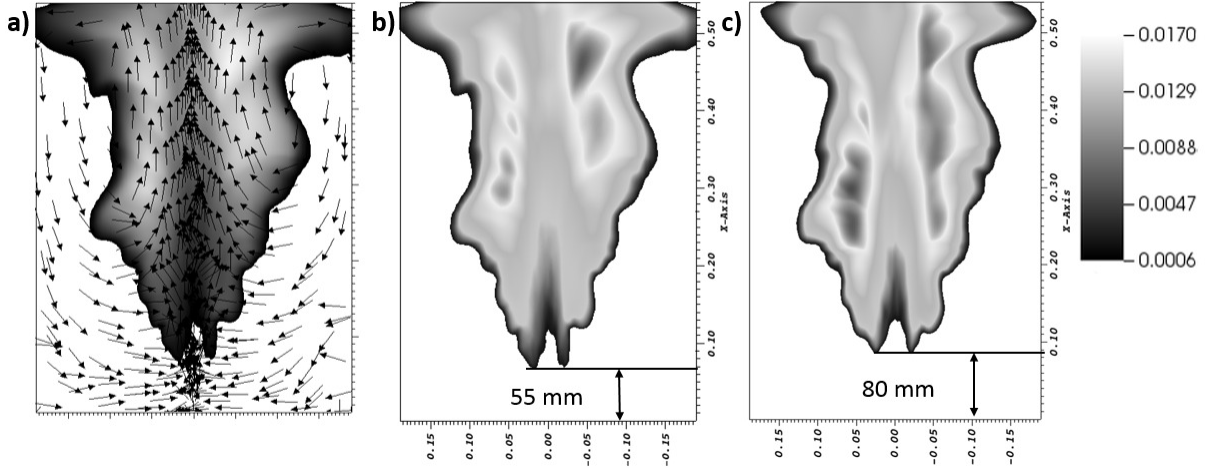


Fig. 3: a) Velocity vector fields (unscaled) in the region of the flame stabilization point superimposed on mean OH field and Mean OH radical contours used to estimate the lift-off height for the predictions obtained by using b) Eq. 5 and c) Eq. 6

distinctive shape of the lifted flame is obtained and the lift-off phenomenon is observed in Fig. 3. Further, the velocity vectors show a clear entrainment of air upstream of the flame stabilization point, which is in agreement with the stabilization mechanism proposed by Broadwell et al. [7]. The lift-off height predictions are estimated according to Cabra et al. [24] criterion, which is the distance between fuel jet and the location of OH mass fraction of 0.0006. As shown in Fig. 3, the predicted lift-off heights are equal to 55 mm and 80 mm using Eq. 5 and Eq. 6, respectively. Therefore, the lift-off height is over-predicted for both SDR models compared to the experimental value of 30 mm. Figure 4 presents the time-averaged methane concentrations from the two sets of LES and the experiments. Reasonable agreement with the experimental values is obtained for both LES calculations with a closer match when Eq. 5 is used, consistent with the lift-off predictions displayed in Fig. 3. Based on these first predictions, the SDR model seems to have an impact on prediction of the methane concentration and lift-off height.

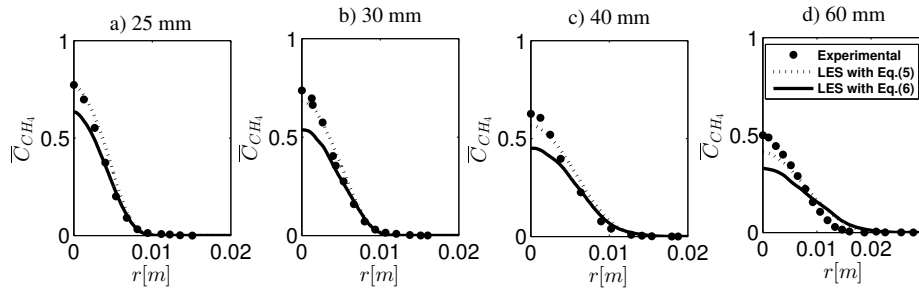


Fig. 4: Comparison between the experimental reacting methane mean concentration profiles at different axial locations downstream of the jet and the numerical predictions obtained by Eq. 5 and Eq. 6.

5 CONCLUSIONS

A numerical investigation of a lifted turbulent jet flame was performed using LES-DCSE developed for partially premixed flames. Good agreement was obtained for non-reacting mean methane concentrations, while the predictions of methane concentration rms profiles need further improvement. This discrepancy may be due to some approximations applied for the turbulence at the fuel inlet. The turbulent lifted flame was reproduced numerically with its distinctive shape. The significance of the sub-grid scale SDR model was assessed by running

two cases with two different SDR models. Based on these preliminary results, the SDR model seems to have an impact on the predictions of lift-off height and the reactive methane concentration. Further work is in progress for finer meshes and improved inlet turbulence boundary conditions.

Acknowledgments

Financial support for this research is provided by the Natural Sciences Engineering Research Council (NSERC) of Canada.

References

- [1] K. M. Lyons, Toward an understanding of the stabilization mechanisms of lifted turbulent jet flames: experiments, *Prog. Energy Combust. Sci.* 33 (2007) 211–231.
- [2] L. Vanquickenborne, A. V. Tiggelen, The stabilization mechanism of lifted diffusion flames, *Combust. Flame* 10 (1966) 59–69.
- [3] H. Eickhoff, B. Lenze, W. Leuckel, Experimental investigations on the stabilization mechanism of jet diffusion flames, *Proc. Combust. Inst.* 20 (1984) 311–318.
- [4] W. M. Pitts, Assessment of theories for the behavior and blowout of lifted turbulent jet diffusion flames, *Proc. Combust. Inst.* 22 (1988) 809–816.
- [5] S. Stárner, R.W. Bilger, J. Frank, D. Marran, M. Long, Mixture fraction imaging in a lifted methane jet flame, *Combust. Flame* 107 (1996) 307–313.
- [6] N. Peters, F. A. Williams, Liftoff characteristics of turbulent jet diffusion flames, *AIAA Journal* 21 (1983) 423–429.
- [7] J. E. Broadwell, W. Dahm, M. G. Mungal, Blowout of turbulent diffusion flames, *Proc. Combust. Inst.* 20 (1984) 303–310.
- [8] K. Watson, K. Lyons, J. Donbar, C. Carter, On scalar dissipation and partially premixed flame propagation, *Combust. Sci. Technol.* 175 (2003) 649–664.
- [9] D. Bradley, P. H. Gaskell, A. K. C. Lau, A mixedness-reactedness flamelet model for turbulent diffusion flames, *Proc. Combust. Inst.* 23 (1990) 685–692.
- [10] C. Müller, H. Breitbach, N. Peters, Partially premixed turbulent flame propagation in jet flames, *Proc. Combust. Inst.* 25 (1994) 1099–1106.
- [11] A. Kronenburg, M. Kostka, Modeling extinction and reignition in turbulent flames, *Combust. Flame* 143 (2005) 342–356.
- [12] D. Dovizio, J. W. Labahn, C. B. Devaud, Doubly conditional source-term estimation DCSE applied to a series of lifted turbulent jet flames in cold air, *Combust. Flame* 162 (2015) 1976–1986.
- [13] D. Dovizio, A. Debbagh, C. Devaud, RANS simulations of a series of turbulent V-shaped flames using Conditional Source-term Estimation, *Flow, Turbul. Combust.* 96 (2016) 891–919.
- [14] D. Dovizio, C. Devaud, Doubly conditional source-term estimation DCSE for the modelling of turbulent stratified V-shaped flame, *Combust. Flame* 172 (2016) 79–93.
- [15] R. W. Schefer, M. Namazian, J. Kelly, Structural characteristics of lifted turbulent-jet flames, *Proc. Combust. Inst.* 22 (1988) 833–842.
- [16] H. Steiner, W. K. Bushe, Large eddy simulation of a turbulent reacting jet with conditional source-term estimation, *Phys. Fluids* 13.
- [17] B. Jin, R. Grout, W. K. Bushe, Conditional source-term estimation as a method for chemical closure in premixed turbulent reacting flow, *Flow, Turbul. Combust.* 81 (2008) 563–582.
- [18] J. Labahn, C. Devaud, Investigation of conditional source-term estimation applied to a non-premixed turbulent flame, *Combust. Theor. Model.* 17 (5) (2013) 960–982.
- [19] K. Bray, M. Champion, P. Libby, N. Swaminathan, Finite rate chemistry and presumed PDF models for premixed turbulent combustion, *Combust. Flame* 46 (2006) 665–673.
- [20] A. Y. Klimenko, Multicomponent diffusion of various admixtures in turbulent flow, *Phys. Fluids A: Fluid Dynamics* 25 (1990) 327–334.
- [21] T. Mantel, R. Borghi, A new model of premixed wrinkled flame propagation based on a scalar dissipation equation, *Combust. Flame* 96 (1994) 443–457.
- [22] H. Kolla, J. W. Rogerson, N. Chakraborty, N. Swaminathan, Scalar dissipation rate modeling and its validation, *Combust. Sci. Technol.* 181 (2009) 518–535.
- [23] S. Pope, U. Maas, Simplifying chemical kinetics: trajectory-generated low-dimensional manifolds, Cornell University Report FDA (1993) 93–11.
- [24] R. Cabra, T. Myhrvold, J. Chen, R. Dibble, A. Karpetsis, R. Barlow, Simultaneous laser Raman-Rayleigh-LIF measurements and numerical modeling results of a lifted turbulent H_2/N_2 jet flame in a vitiated coflow, *Proc. Combust. Inst.* 29 (2002) 1881–1888.